#688

STS-41G
TROPOSPHERIC CO & NO2. MIXING RATIO
84-108A-03A ESAC-00021

STS-51F
MILSTONE DEPLETION EXP.
85-063A-04C
SPMS-00608

Table of Contents

1. Introduction

2. Errata/Change Log

3. LINKS TO RELEVANT INFORMATION IN THE ONLINE NSSDC INFORMATION SYSTEM

4. Catalog Materials

    a. Associated Documents

    b. Core Catalog Materials

---

1. INTRODUCTION:

The documentation for this data set was originally on paper, kept in NSSDC's Data Set Catalogs (DSCs). The paper documentation in the Data Set Catalogs have been made into digital images, and then collected into a single PDF file for each Data Set Catalog. The inventory information in these DSCs is current as of July 1, 2004. This inventory information is now no longer maintained in the DSCs, but is now managed in the inventory part of the NSSDC information system. The information existing in the DSCs is now not needed for locating the data files, but we did not remove that inventory information.

The offline tape datasets have now been migrated from the original magnetic tape to Archival Information Packages (AIP's).

A prior restoration may have been done on data sets, if a requestor of this data set has questions; they should send an inquiry to the request office to see if additional information exists.

2. ERRATA/CHANGE LOG:

NOTE: Changes are made in a text box, and will show up that way when displayed on screen with a PDF reader.

When printing, special settings may be required to make the text box appear on the printed output.

Version	Date	Person	Page	Description of Change
01				
02				

3 LINKS TO RELEVANT INFORMATION IN THE ONLINE NSSDC INFORMATION SYSTEM:

http://nssdc.gsfc.nasa.gov/nmc/

[NOTE: This link will take you to the main page of the NSSDC Master Catalog. There you will be able to perform searches to find additional information]

4. CATALOG MATERIALS:

a. Associated Documents To find associated documents you will need to know the document ID number and then click here.
http://nssdcftp.gsfc.nasa.gov/miscellaneous/documents/

b. Core Catalog Materials

REQ. AGENT

SAR

ACQ. AGENT

CYN

STS-41G

TROPOSPHERIC CO & NO2 MIXING RATIO

84-108A-03A ESAC-00021

This data set consists of 10 9-Track, 6250 BPI, 1 file, ASCII tapes. The D and C tapes and start and stop times are listed below.

D#	C#	TIME SPAN
D-79641	C-27840	10/05/84 - 10/06/84
D-79642	C-27841	10/06/84 - 10/06/84
D-79643	C-27842	10/06/84 - 10/07/84
D-79644	C-27843	10/07/84 - 10/08/84
D-79645	C-27844	10/08/84 - 10/09/84
D-79646	C-27845	10/09/84 - 10/10/84
D-79647	C-27846	10/10/84 - 10/11/84
D-79648	C-27847	10/11/84 - 10/12/84
D-79649	C-27848	10/12/84 - 10/13/84
D-79650	C-27849	10/13/84 - 10/13/84

B R I E F D E S C R I P T I O N

Tropospheric CO & N2O Mix Ratio Tp

84-108A-03A

This set of carbon monoxide and nitrous oxide data was supplied by the principal investigator on magnetic tape in ASCII format. The data set contains carbon monoxide and nitrous oxide volume mixing ratios that were inferred from radiances measured at 2080-2220 cm**-1 wavenumber. About 75,000 individual radiance measurements are obtained over 9 days, covering areas between 57 deg N. and 57 deg S. The column values are retrieved for the altitude range from the top of the mixing layer to the tropopause (3-12 km) and, horizontally, in 5 deg x 5 deg grids. When compared to concurrent aircraft data, the inferred concentrations are systematically low by 20-40%.

M A T E R I A L S F O R D I S T R I B U T I O N

84-108A-03A

Tropospheric CO & N2O Mix Ratio Tp

A description of magnetic tapes: "The Distribution of Middle Tropospheric Carbon Monoxide during Early October 1984", submitted to JGR -- Reprints expected.

A C K N O W L E D G E M E N T S

When using the data in any reports, publications, or presentations, please acknowledge the National Space Science Data Center.

NASA Langley Research Center
Mail Stop 401A
Hampton, VA 23665-5225
May 9, 1989

National Space Science Data Center
Attn: Carolyn Ng
Code 633.8
Goddard Space Flight Center
Greenbelt, MD 20771

RE: Submittal of the MAPS Experiment Data Set from the OSTA-3 Payload Flown on STS-41G in October 1984.

This letter accompanies:

1. 10 magnetic tapes.
2. A description of magnetic tapes.
3. A copy of the paper entitled "The Distribution of Middle Tropospheric Carbon Monoxide During Early October 1984," which has been submitted to JGR.
4. A copy of "Middle and Upper Tropospheric Carbon Monoxide Mixing Ratios as Measured by a Satellite-Borne Radiometer Sensor During November 1981."

1. The magnetic tapes contain all the MAPS instrument and ancillary data needed to reproduce or reanalyze the experimental results to infer carbon monoxide and 2. the current value of the end data product which is the volumatic mixing ratio of carbon monoxide in the middle troposphere. The Description of Magnetic Tapes describes the format of the tapes, the records, and their order as written to the tapes. The paper is a copy of a draft submitted to JGR and contains information addressing points A, B, E, F, I, J, and K on pages 3-5 of NSSDC/WDC-A R&S 84-19. For points G, H and L there are no known unusual events, known anomolies or other conditions affecting the data. If there are further questions call me at 804-864-5366 or 928-5366(FTS).

Sincerely,

W. Andrew Wallio

cc:
401A/CDB
401A/Wallio

DESCRIPTON OF MAGNETIC TAPES

1. Physical record size: 200 characters per record
2. Logical record size: 200 characters per record
3. 9-TRACK tape
4. DENSITY: 6250 bpi
5. UNBLOCKED
6. ODD PARITY
7. UNLABELED
8. ASC II
9. Phase encoding modulation
10. ONE FILE PER TAPE
11. ONE END-OF-FILE PER TAPE

TAPE 1:	START TIME:	279:13:13:00	(24153180. sec.)	NO. RECORDS:	5690
	STOP TIME :	280:00:00:00	(24192000. sec.)		
TAPE 2:	START TIME:	280:00:00:00	(24192000. sec.)	NO. RECORDS:	41393
	STOP TIME :	280:12:00:00	(24235200. sec.)		
TAPE 3:	START TIME:	280:12:00:00	(24235200. sec.)	NO. RECORDS:	41215
	STOP TIME :	281:00:00:00	(24278400. sec.)		
TAPE 4:	START TIME:	281:00:00:00	(24278400. sec.)	NO. RECORDS:	64334
	STOP TIME :	282:00:00:00	(24364800. sec.)		
TAPE 5:	START TIME:	282:00:00:00	(24364800. sec.)	NO. RECORDS:	50724
	STOP TIME :	283:00:00:00	(24451200. sec.)		
TAPE 6:	START TIME:	283:00:00:00	(24451200. sec.)	NO. RECORDS:	7086
	STOP TIME :	284:00:00:00	(24537600. sec.)		
TAPE 7:	START TIME:	284:00:00:00	(24537600. sec.)	NO. RECORDS:	20099
	STOP TIME :	285:00:00:00	(24624000. sec.)		

TAPE 8:	START TIME:	285:00:00:00	(24624000. sec.)	NO. RECORDS:	31277
	STOP TIME :	286:00:00:00	(24710400. sec.)		
TAPE 9:	START TIME:	286:00:00:00	(24710400. sec.)	NO. RECORDS:	78178
	STOP TIME :	287:00:00:00	(24796800. sec.)		
TAPE 10:	START TIME:	287:00:00:00	(24796800. sec.)	NO. RECORDS:	35704
	STOP TIME :	287:15:00:00	(24850800. sec.)		

The data are written with 200 characters per record. The format for reading the records is as follows:

```
     READ (X,N) TIME, TER, LAT, LONG,
*               V, DV, DVP,
*               TBB1, TBB2, TBB4,
*               TBB5, TBB6, TREF,
*               SZN, DNSFT, DNPSFT,
*               N, DN, DNP, CO, N2O,
*               LW, STWD, CDST

     N FORMAT (F10.0, F8.0, 2(F9.2), 3(F8.4), 6(F8.2),
*              3(F7.1), 5(E12.4), I5, 2(I3))
```

NOTE: INTEGER NUMBERS: LW, STWD, CDST

REAL NUMBERS: ALL OTHER VARIABLES

VARIABLE DESCRIPTION:

TIME (F10.0) Time of day in seconds

TIME = DAY * 86400 + HOUR * 3600

+ MINUTES * 60 + SECONDS

TER (F8.0) Mean topographic elevation or bathymetric depths in meters

POSITIVE For Land

NEGATIVE For Water

LAT (F9.2) Degrees

LONG (F9.2) Degrees

V (F8.4)	Measured signal output for the ΔV channel in volts
DV (F8.4)	Measured signal output for the ΔV channel in volts
DVP (F8.4)	Measured signal output for $\Delta V'$ channel in volts
TBB1 (F8.2)	Temperature of controlled internal reference blackbody in degrees Kelvin
TBB2 (F8.2)	Temperature of internal balance blackbody in degrees Kelvin
TBB4 (F8.2)	Temperature of the external calibration blackbody in degrees Kelvin
TBB5 (F8.2)	Temperature of the external balance cold blackbody in degrees Kelvin
TBB6 (F8.2)	Temperature of the external balance hot blackbody in degrees Kelvin
TREF (F8.2)	Temperature of the reference cal cell in degrees Kelvin
SZN (F7.1)	Solar zenith angle in degrees
DNSFT (F7.1)	The signal function weighted atmospheric temperature for the ΔV channel in degrees Kelvin
DNPSFT (F7.1)	The signal function weighted atmospheric temperature for the $\Delta V'$ channel in degrees Kelvin
N (E12.4)	Calculated radiance value for the V channel in watts cm^{-2} SR^{-1}

DN (E12.4) Calculated radiance value for the ΔV channel in watts cm^{-2} sr^{-1}.

DNP (E12.4) Calculated radiance value for the $\Delta V'$ channel in watts cm^{-2} sr^{-1}.

CO (E12.4) Inferred CO mixing ratio for the ΔV channel in parts per billion by volume.

N2O (E12.4) Inferred N_2O mixing ratio for the $\Delta V'$ channel in parts per billion by volume.

LW (I5) Code for terrain type

0 - All positive land

2 - Significant lake included

3 - Contains ice - (no process)

4 - Contains ice - (no process)

5 - Contains land and ocean

8 - Contains some land below sea level

9 - All ocean

STWD (I3) Instrument and mirror status word

STWD = 25 Calibrate/cool balance
= 26 Calibrate/warm balance
= 27 Calibrate/calibrate
= 58 Operate/scene (DATA MODE)
All else mirror moving.

CDST (I3) Inferred CO status word

CDST = 0 Cloud free
= 1 Cloud contaminated
= 2 V channel saturation
= 3 NO TSF data (ZLV off)
= 4 N threshold

CDST (13) Inferred CO status word (Concluded)

CDST = 5 TSF out range
= 6 Terrain type 3 or 4
= 7 CO threshold CO < 0
or CO $\geq$ 240
= 8 Fallout reason
= 9 Calibrate cycle

84-108A-03A

```
$ASS IN HT0
$NOP
$NOP
$NOP
$NOP ********************** TROP1 *********************
$EXE TPLIST BS

INPUT PARAMETERS ARE:  AS FL=1=1 1 1 1

 TAPE NO.   1              FILE NO.   1
 RECORD   1                LENGTH   200
 24153181.     792.     10.28     40.46 -3.3400    .6100    .7400  313.47  282.79  310.57  280.05  320.3
6  293.75    60.5  237.2  238.4    .1350E-04    .1827E-06    .1356E-06   -.9990E+03   -.9990E+03     0 15
 9

 TAPE NO.   1              FILE NO.   1
 RECORD   5960             LENGTH   200
 24191999.   -310.     -9.74  -110.65 -3.0000   1.4100   1.8700  313.34  279.24  310.49  279.84  320.3
2  288.77    68.8  236.9  238.1    .1744E-04    .4245E-06    .3620E-06    .4541E-07    .2148E-06     9 58
 4

***** JOB DONE.
$ASS IN HT1
$NOP
$NOP
$NOP
$NOP ****************** TROP2 ******************
$EXE TPLIST BS

INPUT PARAMETERS ARE:  AS FL=1=1 1 1 1

 TAPE NO.   1              FILE NO.   1
 RECORD   1                LENGTH   200
 24192306.   -3000.    -10.12   -110.42 -3.1000   1.2900   1.8000  313.47  279.24  310.53  279.84  320.2
4  288.77    69.0  236.9  238.1    .1675E-04    .3863E-06    .3469E-06    .4399E-07    .2295E-06     9 58
 6

 TAPE NO.   1              FILE NO.   1
 RECORD  -24143            LENGTH   200
 24235199.     729.     30.66     37.73  -.7500   3.7600   4.4300  313.23  279.56  310.45  280.01  320.3
2  289.15    51.2  236.0  237.1    .3667E-04    .1176E-05    .9256E-06    .5043E-06    .9424E-06     0 58
 1

***** JOB DONE.

$$
$ASS IN HT0
$NOP
```

```
$NOP
$NOP ************** TROP3 ******************
$EXE TPLIST BS

INPUT PARAMETERS ARE:  AS FL=1=1 1 1 1

 TAPE NO.   1              FILE NO.   1
 RECORD   1                LENGTH   200
 24235210.     729.     30.60    37.78  -.8100  3.6800  4.3500  313.22  279.56  310.45  280.01  320.3
2  289.15   51.2  236.0  237.1   .3522E-04   .1150E-05   .9081E-06   .4250E-06   .8292E-06     0 58
 1

 TAPE NO.   1              FILE NO.   1
 RECORD  -24321            LENGTH   200
 24278399.  -5486.     49.79  -172.34 -4.2200   .5500   .7300  313.28  279.64  310.49  280.01  320.3
5  289.15   55.8  231.9  232.6   .6698E-05   .1627E-06   .1187E-06   .1666E-06   .4806E-06     9 58
 1

***** JOB DONE.

$$
$ASS IN HTC
$NOP
```

REQ. AGENT	ACQ. AGENT
SAR	JEJ

STS-51F/SPACELAB 2

DEPLET. EXP MILSTONE. NO1.OMS. 6300A

85-063A-04C SPMS-00608

This data set consists of 1 9-track, 6250 BPI, 1 file, Binary Magnetic tape written in VAX BACKUP FORMAT. The D and C tapes are listed below.

D#	C#
D-78531	C-27850

Boston University

Center for Space Physics
725 Commonwealth Avenue
Boston, Massachusetts 02215

Tel: (617) 353-5990
Telex: 95-1289 BOS UNIV BSN
SPAN: BUASTA::user

8 April 1988

Mr. John Jackson
National Space Science Data Center
Code 633.8
Goddard Space Flight Center
Greenbelt, MD 20771

Dear Mr. Jackson:

Imaging data from the Millstone #1 OMS engine burn were obtained from Horton Point, Long Island, using an intensified all sky CCD camera. The data were taken at 6300Å with a 6Å FWHM filter. The moon was nearly full on the evening of the experiment causing a high background (~20R/Å) that interfered with the weak airglow produced by the burn.

The data supplied is the result of some processing to remove the pre-event airglow and scattered moonlight from the airglow produced by the OMS burn. The data also has been corrected for lens effects and viewing geometry. The data has been remapped on to a geographic grid so as to appear as it would to an observer far above the release altitude. The first image on the data tape is a map overlay to be used with the rest of the images. The images are 512x512 pixels by 8 BITS/pixel. A pixel value of 10 corresponds to a brightness of 0 Rayleighs; a pixel value of 250 represents brightness of 540 Rayleighs over background. Each image is the result of a 20 second integration period. TAble 1 lists the files on the tape and the corresponding start times (U.T.) for each exposure. The tape supplied is a VAX back-up tape whose characteristics are listed on attachment A. Also enclosed is a preprint describing the plasma depletion experiments during the Spacelab-2 mission.

Yours sincerely,

Michael Mendillo
Professor of Astronomy

Enclosure
MM/kac

NSSDC NATIONAL SPACE SCIENCE DATA CENTER

Central Data Services Facility
Operated for NASA by Science Applications Research

Goddard Space Flight Center
Code 633.4
Greenbelt, Maryland 20771
Telephone (301) 286-6695
FTS 888-6695

April 20, 1988

Prof. Michael Mendillo
Boston University
Center for Space Physics
725 Commonwealth Avenue
Boston, Massachusetts 02215

Dear Dr. Mendillo,

Thank you for sending us the imaging data from the Millstone # 1 OMS engine burn, the reprint from Science describing the plasma depletion experiment, and the information contained in your letter.

The National Space Science Data Center I.D. for your experiment is 85-063A-04 and our data set I.D. will most likely be 85-063A-04C, since 04A and 04B have already been assigned to data provided by Dr. P.A. Bernhardt.

The documentation that you sent will most likely meet our requirements. If, however, we have any difficulty reading your tape, we will let you know.

Thank you again for your cooperation.

Sincerely yours,

John E. Jackson

John E. Jackson

```
Listing of save set(s)

Save set:              SPACEL.BCK
Written by:            CHUANG
UIC:                   [000145,000002]
Date:                  16-MAY-1988 12:20:10.07
Command:               BACKUP/LIST=SPACEL.BCK [.*]TR:[CHUANG.SL2]*.* TAPE:SPACEL.BCK
Operating system:      VAX/VMS version V4.6
BACKUP version:        V4.6
CPU ID register:       00000000
Node name:             _BUA:TB::
Written on:            _MSA0:
Block size:            8192
Group size:            10
Buffer count:          3

[CHUANG.SL2]SL.MPx;2
[CHUANG.SL2]SL1.UNW;1
[CHUANG.SL2]SL10.UNW;1
[CHUANG.SL2]SL11.UNW;1
[CHUANG.SL2]SL12.UNW;1
[CHUANG.SL2]SL13.UNW;1
[CHUANG.SL2]SL14.UNW;1
[CHUANG.SL2]SL15.UNW;1
[CHUANG.SL2]SL16.UNW;1
[CHUANG.SL2]SL17.UNW;1
[CHUANG.SL2]SL18.UNW;1
[CHUANG.SL2]SL19.UNW;1
[CHUANG.SL2]SL2.UNW;1
[CHUANG.SL2]SL20.UNW;1
[CHUANG.SL2]SL21.UNW;1
[CHUANG.SL2]SL22.UNW;1
[CHUANG.SL2]SL23.UNW;1
[CHUANG.SL2]SL24.UNW;1
[CHUANG.SL2]SL25.UNW;1
[CHUANG.SL2]SL26.UNW;1
[CHUANG.SL2]SL27.UNW;1
[CHUANG.SL2]SL28.UNW;1
[CHUANG.SL2]SL29.UNW;1
[CHUANG.SL2]SL3.UNW;1
[CHUANG.SL2]SL30.UNW;1
[CHUANG.SL2]SL31.UNW;1
[CHUANG.SL2]SL32.UNW;1
[CHUANG.SL2]SL33.UNW;1
[CHUANG.SL2]SL34.UNW;1
[CHUANG.SL2]SL4.UNW;1
[CHUANG.SL2]SL5.UNW;1
[CHUANG.SL2]SL6.UNW;1
[CHUANG.SL2]SL7.UNW;1
[CHUANG.SL2]SL8.UNW;1
[CHUANG.SL2]SL9.UNW;1

Total of 35 files, 17020 blocks
End of save set
```

Reprint Series
27 November 1987, Volume 238, pp. 1260–1264

SCIENCE

85-063A-04

Spacelab-2 Plasma Depletion Experiments for Ionospheric and Radio Astronomical Studies

M. MENDILLO, J. BAUMGARDNER, D. P. ALLEN, J. FOSTER, J. HOLT, G. R. A. ELLIS, A. KLEKOCIUK, AND G. REBER

Copyright © 1987 by the American Association for the Advancement of Science

Spacelab-2 Plasma Depletion Experiments for Ionospheric and Radio Astronomical Studies

M. MENDILLO, J. BAUMGARDNER, D. P. ALLEN, J. FOSTER, J. HOLT, G. R. A. ELLIS, A. KLEKOCIUK, G. REBER

The Spacelab-2 Plasma Depletion Experiments were a series of studies to examine shuttle-induced perturbations in the ionosphere and their application to ground-based radio astronomy. The space shuttle Challenger fired its orbital maneuvering subsystem engines on 30 July and 5 August 1985, releasing large amounts of exhaust molecules (water, hydrogen, and carbon dioxide) that caused the electrons and ions in Earth's upper atmosphere to chemically recombine, thereby creating so-called "ionospheric holes." Two burns conducted over New England produced ionospheric peak depletions ranging from 25 to 50 percent, affected the ionosphere over a 200-kilometer altitude range, and covered 1° to 2° of latitude. Optical emissions associated with the hole spanned an area of several hundred thousand square kilometers. A third burn was conducted over a low-frequency radio observatory in Hobart, Australia, to create an "artificial window" for ground-based observations at frequencies normally below the natural ionospheric cutoff (penetration) frequency. The Hobart experiment succeeded in making high-resolution observations at 1.7 megahertz through the induced ionospheric hole.

THE SPACELAB-2 PLASMA DEPLETION Experiments conducted by the space shuttle Challenger from 29 July to 5 August 1985 represented an innovative use of the shuttle to perform space physics experiments in Earth orbit. For the first time in the shuttle program, the orbiter's small onboard engines (called the Orbital Maneuvering Subsystem or OMS engines) were fired for reasons other than to change the shuttle's orbit. These scientifically dedicated OMS firings were used to conduct a series of "active space plasma experiments" in which large quantities of neutral gases were injected into the ionosphere.

The OMS exhaust gases (H_2O, H_2, and CO_2) react rapidly with the ambient ionospheric plasma, causing the dominant atomic ions (O^+) to be converted to molecular ions (H_2O^+, OH^+, and O_2^+), which then recombine very rapidly with the ambient electrons (e^-) to form neutral species that yield optical emissions. The end result is to cause a sudden depletion in the local plasma concentrations, the creation of a so-called "ionospheric hole" (*1–3*).

The reasons for introducing such a well-defined stress into the ionosphere fall into three broad areas: (i) All shuttle missions use OMS burns for orbit insertion, for changes of orbit during a mission, and for deorbit. The prediction that ionospheric holes occur with each such maneuver needed to be verified for operational and environmental reasons. (ii) The creation of an ionospheric hole, performed in conjunction with a multidiagnostic observing program, allows one to study the "system response function" of the upper atmosphere. Earth's plasma environment involves a complex mix of processes linking solar ionizing radiation, chemical reactions between many ionized and neutral components of the atmosphere, dynamic properties (for example, winds and diffusion) of the upper atmosphere, and electrodynamic processes imposed by electric and magnetic fields of terrestrial and solar wind origin. By introducing known perturbations into a well-defined subsystem and measuring the response, we can apply standard laboratory techniques to Earth's plasma environment. Such input-output tests, coupled to computer models of the overall system, form the essence of what is meant by the phrase "active experiments" in space. (iii) Artificially induced plasma depletions, once understood and capable of being modeled in detail, can then be used to instigate other space plasma phenomena, such as the growth of plasma instabilities or the modification of radio propagation paths, thus introducing a second level of laboratory-in-space experimentation to the space sciences (*4*).

The concept behind using a Spacelab mission to investigate both the basic plasma physics and applications areas of ionospheric holes was that a shuttle mission dedicated completely to space science had the unique ability to control all aspects of the vehicle's orbit. This requirement was of crucial importance because ionospheric holes are effects left literally in the wake of the shuttle, and thus all major observations had to be made from well-equipped ground-based observatories. The OMS burns had to be conducted at certain altitudes, with precise ground tracks, and within certain local time windows and specified lunar lighting conditions.

The burns for the three experiments (Millstone 1, Millstone 2, and Hobart) are

M. Mendillo, J. Baumgardner, D. P. Allen, Department of Astronomy, Boston University, Boston, MA 02215.
J. Foster and J. Holt, Massachusetts Institute of Technology, Haystack Observatory, Westford, MA 01886.
G. R. A. Ellis, A. Klekociuk, G. Reber, Department of Physics, University of Tasmania, Hobart, Tasmania, Australia.

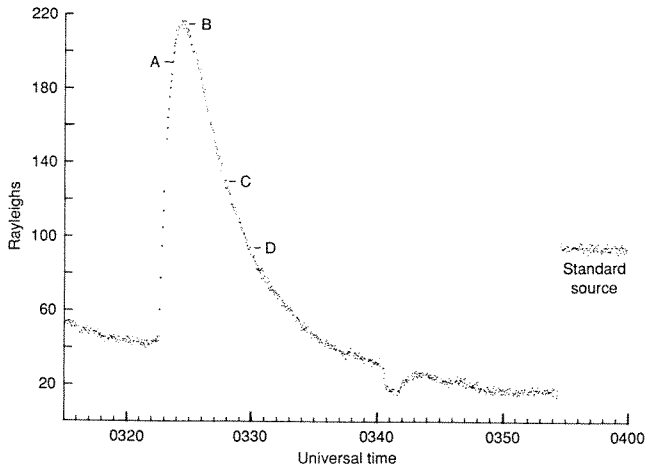

Fig. 1. Airglow observations at 6300 Å obtained with a 1° photometer at Horton Point, Long Island, pointed toward the center of the Millstone Hill nighttime OMS burn experiment on 30 July 1985. The points marked (A) through (D) indicate the times for simultaneous imaging results shown in Fig. 2 and are as follows: A, 0323:33 UT; B, 0325:02 UT; C, 0328:00 UT; and D, 0329:50 UT.

named by the major radio observatory associated with each experiment. The Millstone Hill Incoherent Scatter Radar is part of the Massachusetts Institute of Technology Haystack Observatory in Westford, Massachusetts (42.62°N, 70.48°W). An incoherent scatter radar is one of the major observational tools for ionospheric physics (*5*). Pulsed ultrahigh-frequency transmissions returned from the ionosphere provide line-of-sight observations of the local electron and ion densities, their temperatures, and the overall bulk plasma drift. Separate nighttime (Millstone 1) and daytime (Millstone 2) OMS burns were conducted to investigate the formation and evolution of ionospheric depletions under significantly different conditions. The nighttime experiment used a 47-second OMS burn (during which the shuttle moved 360 km), releasing almost 830 kg of exhaust gases into the ionosphere (*6*). It was conducted after sunset in order to avoid simultaneous solar re-ionization of the atmosphere. The Millstone 1 experiment was thus designed to produce the largest and most long-lived ionospheric hole that might be caused by the shuttle. In contrast, the Millstone Hill 2 burn was conducted in mid-afternoon with a 6-second burn of a single OMS engine to release <10% of the molecules available for Millstone Hill 1 (68 kg) (*7*). Millstone 2 should help to define the lower limits of shuttle-induced ionospheric holes. In both cases, the OMS burns were placed south of the Millstone antenna in order to have the radar's ray path essentially parallel to the geomagnetic field lines, thereby maximizing the chance of measuring Doppler shifts from plasma diffusion along magnetic field lines into the depleted regions.

For the Hobart OMS burn, a different set of criteria prevailed. The goal of the experiment was to test the concept of conducting low-frequency radio astronomy through an artificially created ionospheric window (*8*). Cosmic radio signals in the 1- to 3-MHz band, synchrotron radiation from the interstellar medium, or discrete sources of planetary origin (for example, Jupiter's magnetosphere) are normally below the radio penetration frequency imposed by the ionospheric plasma. These signals are thus reflected back into space by the ionospheric electrons just as terrestrial signals in the same band are reflected back toward Earth, thereby making possible long-distance radio communication. The low-frequency radio observatory operated by the University of Tasmania in Hobart, Tasmania, Australia (42.30°S, 212.97°W), has conducted ground-based observations in the low-frequency domain from a site where the ionosphere is often naturally weak (the so-called mid-latitude trough). For the Spacelab-2 experiment, the OMS burn was conducted under near optimal conditions: predawn, winter-nighttime, solar minimum conditions, with the burn virtually above the antenna (*9*).

The large OMS burn across southern New England on the night of 29 July 1985 was monitored by a network of radio and optical diagnostic systems. During the subsequent burn of 4 August 1985, conducted in full daylight, observations were limited to the Millstone radar. Optical measurements (photometer and imaging systems) are used in ionospheric depletion experiments to record the 6300-Å airglow induced by the recombination chemistry that forms the hole. The red emission comes mainly from the CO_2 branch of the OMS-initiated chemistry. The dissociation of O_2^+ with electrons results in one or both of the oxgen atoms left in the ^1D state, with a radiative lifetime of 147 seconds. Optical emissions thereby map the recent occurrence of plasma depletions.

To observe the 6300-Å cloud emitted by the Millstone 1 shuttle burn, Boston University's Mobile Ionospheric Observatory (MIO) was deployed to Horton Point, Long Island, a site selected because of its proximity to the burn track and a forecast for clear skies there on the day of the experiment. Figure 1 shows the temporal pattern obtained with the 1° photometer in the MIO pointed to the center of the burn. Before the event, ambient airglow levels showed a gradual decline typical of summer post-sunset (2200 local time) ionospheric decay. Within seconds of the OMS burn, the 6300-Å signal increased sharply, reaching a maximum at ~2 minutes after the end of the OMS burn. The subsequent decay to pre-event levels took approximately 15 minutes. The airglow levels shown in Fig. 1 are well below the brightness levels required for visual observations. An image-intensified charge-coupled device (CCD) camera system can readily record such levels with an all-sky (fish-eye) lens (*10*). Figure 2 contains a summary of four images taken from the MIO on Horton Point that describe the spatial extent of the airglow cloud at the four times indicated on the photometer curve in Fig. 1. Although these images were taken from the ground, they have been transferred onto a geographic map by using an emission height corresponding to the shuttle's altitude (320 km) at the time of the burn. Also included on each frame are the OMS burn path, the MIO and Millstone Hill observation sites, the photometer monitoring point, and the ray path from the Millstone Radar, the latter two aimed at the burn center.

The images in Fig. 2 show an airglow cloud that begins as an elongated feature; these images reveal depletions formed by the OMS gases while they are still close to the shuttle trajectory. During the next few minutes, the effect spreads through the ionosphere as the molecules diffuse rapidly through the rarefied upper atmosphere. At the time of peak brightness [0325:02 universal time (UT)], the effect spans >300 km. In its later stages, the faint airglow cloud is nearly circular, covering ~400,000 km^2.

Several dynamic effects are evident in Fig. 2. The center of the airglow cloud is clearly displaced by ~150 km from the center of the OMS burn. This is due to the fact that the exhaust cloud shares in the shuttle's forward motion. With an orbital speed of ~8 km sec^{-1} toward the southeast, and the OMS exhaust gases at ~3 km sec^{-1} to the northwest, the molecules enter the ionosphere at ~5 km sec^{-1} in the direction of the shuttle's motion. Owing to the low atmospheric densities at 320 km altitude, $[O] = 1.3 \times 10^8$ cm^{-3} for a neutral temperature of 743 K (*11*), collisions occur at a frequency of ~0.1 sec^{-1}, and thus the forward motion of the cloud is stopped in about three collisions.

Figure 3 contains a summary of the changes in the electron density altitude profiles, $n_e(h)$, observed by the Millstone Hill radar during the formation stage of the hole. With the antenna pointed at elevation 56° and azimuth 179°, the beam crossed the shuttle altitude at the center of the burn. Note, therefore, that electron density values at altitudes <320 km come from regions below and to the north of the intersection point, whereas n_e for altitudes >320 km pertain to regions south of the intersection point. Individual electron density profiles were taken with a 20-second integration time and a pulse length of 48 km in slant range. Thus, the 1° beam of the antenna gives a 7 by 7 by 48 km^3 slice through the ionosphere at the range corresponding to the intersection point (~385 km). Because of the low signal-to-noise values associated with such an experiment, several individual profiles were averaged to give the mean evolution patterns shown in Fig. 3A.

During the first minute after the shuttle passed through the radar beam (Fig. 3B), one can see that a large depletion was readily detected. This ~45% hole in the local plasma density is flanked by small enhancements (~10%) above and below the core depletion. These enhancements are believed to be due to a physical displacement of plasma by the shuttle and its exhaust gases, the so-called "snowplow effect" associated with the injection of a dense gas into a plasma (*4, 12, 13*). This early-phase effect is quickly overpowered by recombination chemistry as the molecules begin to diffuse through the ionosphere. In Fig. 3C the hole is well formed, corresponding in time to the peak airglow production time in Figs. 1 and 2. In Fig. 3D, the hole is seen to recover somewhat at the center, to broaden in its altitude extent, and to have the peak depletions occur at lower altitudes. This pattern essentially marks the end of the rapid hole-making stage. Reacting to the strong gradients produced by the initial burst of chemistry, plasma now diffuses into the hole from above and below. Simultaneously, the heavy exhaust gases sink to lower ionospheric heights, causing further depletions. The airglow results show that this process continued for about 15 to 20 minutes.

Figure 3 also shows the electron density profile results obtained during the initial phase of the daytime Millstone burn. With the radar pointed at elevation 62° and azimuth 169°, and the burn placed to the west of the orbit-radar intersection point because of the slippage effect seen in Fig. 2, the resultant perturbations are seen to be remarkably similar in form, but reduced in magnitude, to the nighttime effects. The differences in depth can be related to the smallness of the burn and the replenishment of the ionosphere by solar ionizing radiation.

After the nighttime fixed-position observations shown in Fig. 3 were made, the Millstone radar conducted a series of elevation scans at the same azimuth in order to map the altitude-latitude extent of the hole.

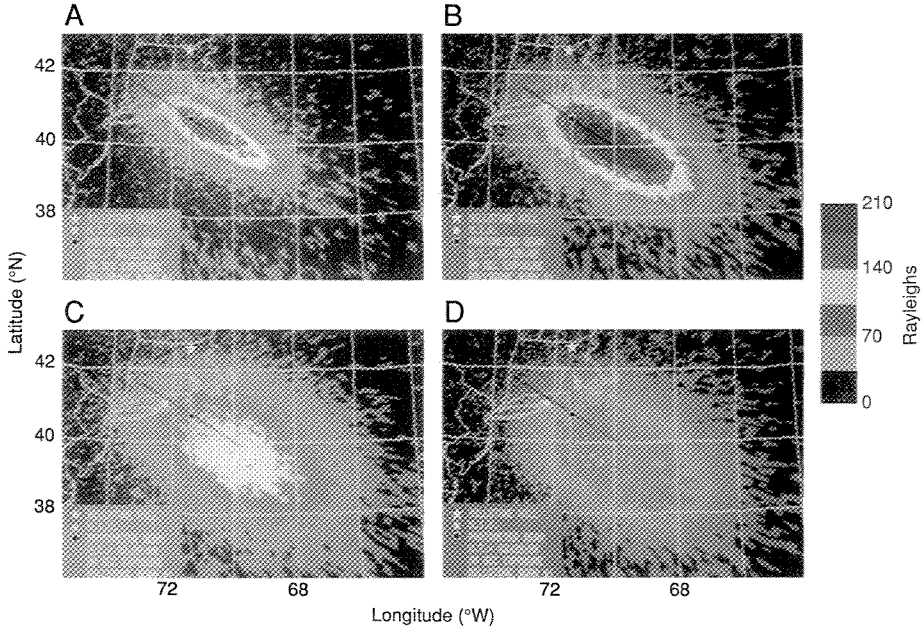

Fig. 2. Summary of four optical images (6300 Å) for the Millstone Hill nighttime experiment obtained with a CCD camera at Horton Point, Long Island. The optical emission comes from the neutralization of ionospheric ions and electrons caused by the CO_2 in the shuttle's exhaust. Each image is a 20-second exposure. The times of the images (as indicated on the photometer curve in Fig. 1) are (**A**) 0323:33 UT, (**B**) 0325:02 UT, (**C**) 0328:00 UT, and (**D**) 0329:50 UT. The photometer results in Fig. 1 give the induced 6300 Å on a background of ~40 rayleighs, but the images in this figure have the background levels subtracted. The symbols on the images indicate the following: star, the Millstone Hill site; circle, the MIO site; and square, the photometer monitoring point.

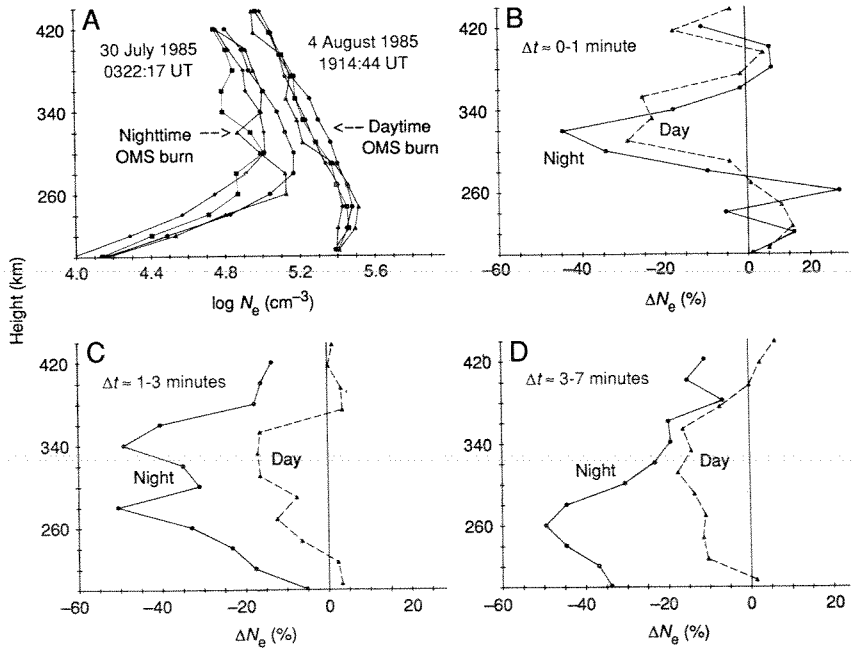

Fig. 3. Summary of early-time electron density variations observed by the Millstone Hill radar for both the night and day experiments. For the nighttime burn, the radar was held fixed at the elevation and azimuth corresponding to the center of the burn shown in Fig. 2. For the daytime experiment, the radar beam crossed the shuttle altitude at the elevation and azimuth corresponding to the end point of the OMS engine burn. (**A**) Nighttime and daytime electron density profiles; (**B**) electron density percentage differences during the first minute after the burns; (**C**) electron density percentage differences at 1 to 3 minutes after the burns; and (**D**) electron density percentage differences at 3 to 7 minutes after the burns.

Sample results from this mode give "late-time" effects that are shown in Fig. 4. The $n_e(h)$ versus latitude pattern seen in Fig. 4A is approximately 32 minutes before the experiment. The scan taken ~14 minutes after the burn (Fig. 4B) reveals a well-formed trough spanning about 1° of latitude. Forty minutes after the burn (Fig. 4C), a well-formed depletion duct continues to be observed. Observations in Fig. 4D, some 107 minutes after the burn, suggest a weak but lingering signature of the hole.

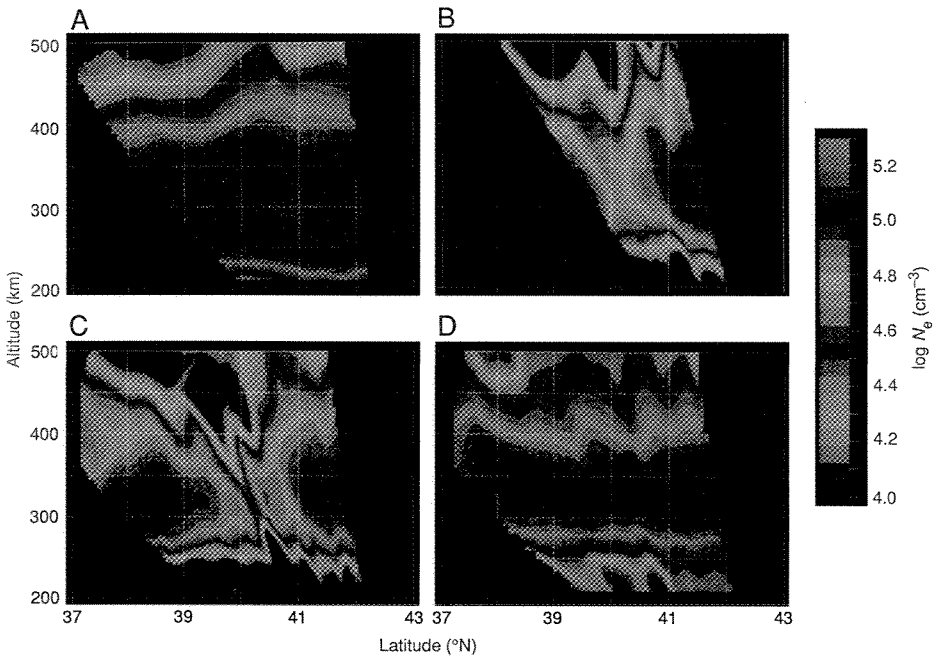

Fig. 4. Summary of the late-time electron density variations observed during the Millstone Hill nighttime experiment on 30 July 1985. The antenna was scanned in elevation angle to map the latitude-altitude structure of the hole. The panels show (**A**) conditions before the event (0247:41 to 0253:23 UT) and the resultant perturbations at (**B**) ~+14 minutes (0335:26 to 0338:56 UT), (**C**) ~+40 minutes (0359:19 to 0404:58 UT), and (**D**) ~+107 minutes (0506:47 to 0512:26 UT). The algorithm used to edit and smooth the radar observations tends to accentuate wavelike patterns in the raw data.

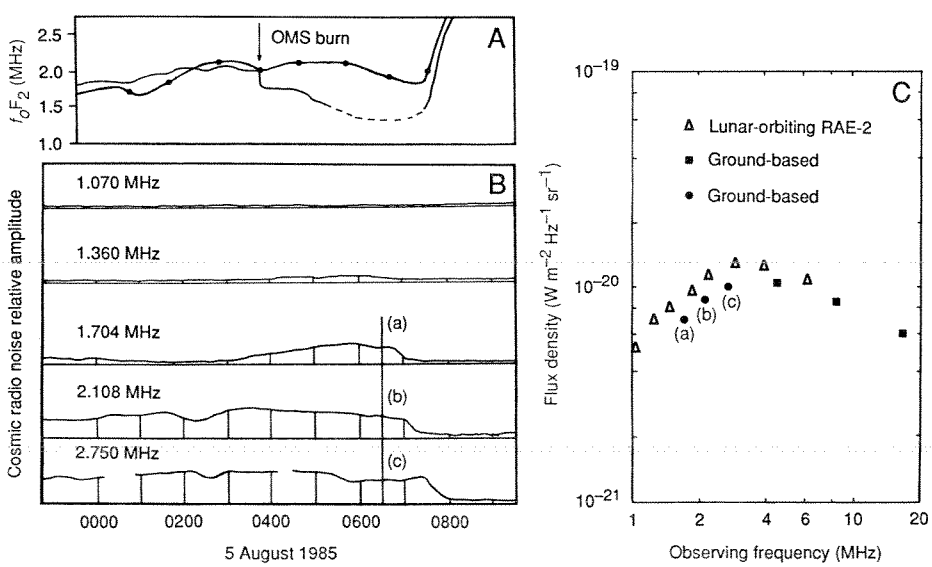

Fig. 5. (**A**) The behavior of the ionospheric penetration frequency (f_oF_2) recorded by an ionosonde in Hobart (solid and dashed line) and a control curve of hourly f_oF_2 values (filled circles) recorded in Melbourne (more than 500 km from the Hobart site). The dashed portion of the Hobart f_oF_2 curve from 0500 to 0700 UT expresses uncertainties in the very low f_oF_2 values. (**B**) Cosmic radio noise levels at various frequencies observed on the night of 5 August 1985 at the University of Tasmania Radio Observatory in Hobart. Times are in local time (LT), corresponding to UT plus 10 hours. (**C**) Galactic radio spectrum on a log frequency scale observed at 0630 LT (filled circles) by means of the observations at (a) 1.704 MHz, (b) 2.108 MHz, and (c) 2.750 MHz from (B). Additional ground-based observations (filled squares) at 4.7, 8.3, and 16.5 MHz are also shown (*19*). For comparison, the low-resolution spectrum observed by the lunar-orbiting spacecraft RAE-2 for the south galactic pole region is also shown (open triangles) (*18*).

A comparison of the airglow images in Fig. 2 and the latitude patterns in Fig. 4 points out that the radar scans did not cut through the exact center of the hole because of the exhaust slippage effect. The peak airglow brightness level in the images reached about 200 rayleighs (where 1 rayleigh is 10^6 photons per square centimeter per second), approximately 18% higher than the peak value seen where the photometer and radar were aimed. This relatively small difference in airglow would not be associated with additional depletions of comparable size. We thus believe that the radar data give a fairly accurate portrayal of the maximum size and depth of the ionospheric hole, in spite of the fact that the scan was not precisely through the hole center.

The images in Fig. 2 also suggest that the airglow cloud moved somewhat to the south (that is, in the last frame the line of symmetry is no longer along the burn trajectory). The radar data at late times (Fig. 4) do not show a significant displacement of the plasma hole. Such differences are probably related to the fact that atmospheric winds can move neutral species [for example, CO_2 and $O(^1D)$] horizontally (across magnetic field lines), whereas plasma is constrained to move essentially vertically (along the field lines).

To test the concept of opening a window for ground-based low-frequency radio astronomy, a 244-kg OMS burn was conducted over the University of Tasmania's radio observatory in Hobart. Pioneering efforts in low-frequency work have been conducted at that site during solar minimum years when the ionosphere is naturally weak (*14, 15*). The Spacelab-2 mission occurred during a period of very low solar activity, during a winter, predawn period in the Southern Hemisphere, conditions when the ionosphere is transparent to all but the lowest radio frequencies (f <2 MHz). The full set of diagnostic instruments and observations made during the Hobart experiment are described elsewhere (*16*).

After the shuttle engine burn, the F-region's peak electron density was reduced by approximately 30%, thereby lowering the penetration frequency (f_oF_2) from ~2.0 to ~1.7 MHz (Fig. 5A). Cosmic radio noise was monitored at a series of frequencies (1.070, 1.360, 1.704, 2.108, and 2.750 MHz) before and after the burn (Fig. 5B). The signals at 1.07 and 1.36 MHz remained unchanged since the electron densities in the depleted ionosphere were still too high to permit reception; at 2.1 and 2.8 MHz, the

received signals were unchanged since these frequencies were already above the penetration frequency. At 1.7 MHz, however, the transition occurred from no reception to reception. This is consistent with earlier observations that showed that the galactic signal normally begins leaking through the ionosphere when f_oF_2 falls to within about 100 kHz of the receiver frequency (*14*). The signal reached a maximum at 0540 hours and then slowly decreased until sunrise caused f_oF_2 to rise near 0700 hours. The profile from 0540 to 0640 hours was generally similar to that at 2.108 MHz and to the corresponding variation seen at the same right ascension in previous observations at 2.13 MHz (*17*) and may be taken to represent the galactic brightness distribution of declination −43° and right ascension of 0200 to 0300 hours. This is the first observation of this region at 1.7 MHz with 25° resolution, the nearest similar measurements having been made with the lunar-orbiting spacecraft RAE-2 at 1.3 MHz and with 130° resolution (*18*).

Figure 5C shows the spectrum of the galactic background radio emission derived from the observations at 0630 local time (galactic coordinates $\ell = 220°$, $b = -52°$). The spectrum observed by the RAE-2 spacecraft is shown for comparison. The flux measurement labeled (a) at 1.704 MHz represents the view through the "ionospheric hole" associated with the shuttle-induced plasma depletion. Observations over a period of several weeks before and after the experiment failed to produce any comparable records at 1.704 MHz since the natural ionospheric cutoff frequency never approached the low values associated with the Spacelab-2 "ionospheric hole" experiment.

The Millstone Hill experiments provided clear and unambiguous documentation of both the largest and smallest types of ionospheric holes capable of being induced by the space shuttle OMS engines. Although full modeling results are yet to be completed, the observations are essentially consistent with theories before the experiment. The sizes and longevities of the holes were somewhat larger and longer than anticipated, and the airglow patterns still require detailed simulation work to verify the dominant chemistry tracks. The dramatic slippage of the exhaust cloud through the ionosphere demonstrates the need for precise planning for future active experiments requiring gas releases at orbital speeds. In addition, the Hobart experiment succeeded in demonstrating that artificial means can be used to open ionospheric windows for the reception of low-frequency radiation of celestial origin.

REFERENCES AND NOTES

1. M. Mendillo and J. M. Forbes, *J. Geophys. Res.* **83**, 151 (1978).
2. P. A. Bernhardt, *ibid.* **84**, 793 and 4341 (1979).
3. M. Mendillo, *Adv. Space Res.* **1**, 275 (1981).
4. ———, *ibid.*, in press.
5. J. V. Evans, *Proc. IEEE* **57**, 496 (1969).
6. The Millstone 1 nighttime burn occurred from 0322:17 to 0323:04 UT on 30 July 1985 at an altitude of 320 km from 41.6°N, 73.1°W to 40.0°N, 69.8°W.
7. The Millstone 2 daytime burn occurred from 1914:44 to 1914:50 UT on 4 August 1985 at an altitude of 323 km from 40.9°N, 71.5°W to 41.1°N, 71.1°W.
8. M. D. Papagiannis and M. Mendillo, *Nature (London)* **255**, 42 (1975).
9. The Hobart burn occurred from 1659:27 to 1659:43 UT on 4 August 1985 at an altitude of 322 km from −42.4°N, 213.5°W to −42.9°N, 212.3°W.
10. J. Baumgardner and S. Karandanis, *Electron. Imaging* **3**, 28 (1984).
11. A. E. Hedin, *J. Geophys. Res.* **88**, 10170 (1983).
12. H. G. Booker, *ibid.* **66**, 1073 (1961).
13. R. H. Wand and M. Mendillo, *ibid.* **89**, 203 (1984).
14. G. Reber and G. R. A. Ellis, *ibid.* **61**, 1 (1956).
15. G. R. A. Ellis, *Mon. Notices R. Astron. Soc.* **130**, 429 (1965).
16. G. R. A. Ellis *et al.*, *Adv. Space Res.*, in press.
17. G. Reber, *J. Franklin Inst.* **285**, 1 (1967).
18. J. C. Novaco and L. W. Brown, *Astrophys. J.* **221**, 114 (1978).
19. G. R. A. Ellis, *Aust. J. Phys.* **35**, 91 (1982).

20. We thank the Spacelab-2 crew, NASA team members at the Marshall Space Fight Center (with special thanks to S. Perrine and the Orbital Dynamics Group), and many colleagues who contributed to these experiments. Funding for this work came in part from NASA contract NAS8-32844 to Boston University. The Millstone radar program was supported under NSF Cooperative Agreement ATM-84-19117 to the Massachusetts Institute of Technology. The University of Tasmania radio astronomy observations were financed by the Australian Research Grant Scheme.

26 May 1987; accepted 22 September 1987

```
$END  LEVELS
DATA IGNORED
$/R
NO PROCEDURE
DATA IGNORED
$ASS IN TA1
$NOP
$NOP
$NOP
$NOP
$NOP
$NOP ================================ LIST OF DEPL1 ==============================
$EXE TPLIST BS

INPUT PARAMETERS ARE:  AS AL 1 1 1

 TAPE NO.   1              FILE NO.   1
 RECORD   1                LENGTH   80
VOL1SPACE                                                                  3

 TAPE NO.   1              FILE NO.   1
 RECORD   2                LENGTH   80
HDR1SPACEL.BCK        SPACE 0001 0001 0001 00 88075 00000 000000DECVMSBACKUP

 TAPE NO.   1              FILE NO.   1
 RECORD   3                LENGTH   80
HDR2F 0819208192                    M              00

***** JOB DONE.
$EXE TPLIST BS

INPUT PARAMETERS ARE:  AS AL 1 1 3

 TAPE NO.   1              FILE NO.   3
 RECORD   1                LENGTH   80
EOF1SPACEL.BCK        SPACE 0001 0001 0001 00 88075 00000 001325DECVMSBACKUP

 TAPE NO.   1              FILE NO.   3
 RECORD   2                LENGTH   80
EOF2F 0819208192                    M              00

***** JOB DONE.
$EXE TPDUMP BS
```

DUMP OF TAPE DEPL1

INPUT TAPE DEPL1 ON TA1
DATA INPUT H9 NF 2 SR 2 1 1 SR 2 LAST 1

FILE	INPUT RECS.	DATA RECORDS INPUT	MAX. SIZE	READ ERROR SUMMARY PERM	ZERO B	SHORT	UNDEF.	INPUT RETRIES #RECS.	TOTAL#
1	3	3	8192	0	0	0	0	0	0

FILE 2 RECORD 1 LENGTH 8192BYTES

(0)	00010004	01000100	01000000	00000000	00000000	00000000	00000000	00000000	01010100	8BE3C633
(40)	002 0014	00000110	3A535041	43454C2E	42434B00	10000000	00000000	00000000	00000000	00000000
(80)	000 0000	00000000	00000000	00000000	00000000	00000000	00000000	00000000	00000000	00000000
(120)	000 0000	00000000	00000000	00000000	00000000	00000000	00000000	00000000	00000000	00000000
(160)	00000000	00000000	00000000	00000000	00000000	00000000	00000000	00000000	00000000	00000000
(200)	000 0000	00000000	00000000	00000000	00000000	00000000	00000000	00000000	00000000	00000000
(240)	000 0000	00000000	00000000	0003A62	C0000100	00000000	00000000	00000000	01010A00	01005350
(280)	4143454C	2E424343	3B000200	42414343	55502F4C	49535430	53504143	454C2E42	43432041	53545234
(320)	5B434855	414E472E	534C325D	2A2E2A20	54415045	3A535041	43454C2E	42434B0C	00040043	4855414E
(360)	472 2424	2424242	0145000	0045 0008	00000E0	9D432DD2	FD900002	00070000	04040008	00563420
(400)	36090009	005F4255	41535442	3A3A0400	0A000000	00080600	03005F4D	5341303A	04000C00	56342E35
(440)	0400D 00	002 00000	02000500	6A000200	0F000300	00000000	F0000300	00000000	00000000	00000000
(480)	010114 00	2A005B43	4855414E	472E534C	325D534C	2E4D5058	3B320200	2B000102	06002C00	A83A0600
(520)	010 0400	2E000102	00000400	2F000200	45002000	34000100	00020000	01020000	01020000	00000002
(560)	00000000	00000000	00000000	00000600	2D00A63A	05000000	02003000	00FF0200	31000000	01003200
(600)	10040033	01000100	0042004B	00FF7F01	00500000	01005700	0004004F	00020200	00020035	00020008
(640)	0036 018	508C2AC9	4C8F 018	10370020	FB8AD2E1	4C8F0008	00380000	00000000	00000008	00390000
(680)	000 0001	00000004	0047 002	00450002	00480088	34020044	00000000	00000000	00000000	00000000
(720)	001C0400	00000000	01000000	00000000	00000000	00000000	00000000	00000000	00000000	00000000
(760)	000 0000	10000000	00000010	00000000	00000000	40000000	00000000	00000000	00000000	00000000
(800)	000 0000	00000000	00000000	00000000	00000000	00000000	00000000	00000000	00000000	00000000
(840)	00000000	00000000	00000000	00000000	00000000	00000000	00000000	00000000	00000000	00000000
(880)	00000000	10000000	00000000	00000000	00000000	00000000	00000000	00000000	00000000	00000000
(920)	000 0000	00000000	00000000	00000000	00000000	00000000	00000000	00000000	00000000	00000000
(960)	000 0000	00000000	00000000	00000000	00000000	00000000	00000000	00000000	00000000	00000000
(1000)	00000000	00000000	00000000	00000000	00000000	00000000	00000000	00000000	00000000	00000000
(1040)	000 0000	10000000	00000000	00000000	00000000	00000000	00000000	00000000	00000000	00000000
(1080)	000 0000	00000000	00000000	00000000	00000000	00000000	00000000	00000000	00000000	00000000
(1120)	000 0000	00000000	00000000	00000000	00000000	00000000	00000000	00000000	00000000	00000000
(1160)	00000000	00000000	00000000	00000000	00000000	00000000	00000000	00000000	00000000	00000000
(1200)	000 0000	10000000	00000000	00000000	00000000	00000000	00000000	00000000	00000000	00000000
(1240)	000 0000	00000000	00000000	00000000	00000000	00000000	00000000	00000000	00000000	00000000
(1280)	00000000	00000000	00000000	00000000	00000000	00000000	00000000	00000000	00000000	00000000
(1320)	000 0000	10000000	00000000	00000000	00000000	00000000	00000000	00000000	00000000	00000000
(1360)	000 0000	00000000	00000000	00000000	00000000	00000000	00000000	00000000	00000000	00000000
(1400)	000 0000	00000000	00000000	00000000	00000000	00000000	00000000	00000000	00000000	00000000
(1440)	00000000	00000000	00000000	00000000	00000000	00000000	00000000	00000000	00000000	00000000
(1480)	000 0000	10000000	00000000	00000000	00000000	00000000	00000000	00000000	00000000	00000000
(1520)	000 0000	00000000	00000000	00000000	00000000	00000000	00000000	00000000	00000000	00000000
(1560)	000 0000	00000000	00000000	00000000	00000000	00000000	00000000	00000000	00000000	00000000
(1600)	000 0000	00000000	00000000	00000000	00000000	00000000	00000000	00000000	00000000	00000000
(1640)	000 0000	00000000	00000000	00000000	00000000	00000000	00000000	00000000	00000000	00000000
(1680)	000 0000	00000000	00000000	00000000	00000000	00000000	00000000	00000000	00000000	00000000
(1720)	00000000	00000000	00000000	00000000	00000000	00000000	00000000	00000000	00000000	00000000
(1760)	000 0000	00000000	00000000	00000000	00000000	00000000	00000000	00000000	00000000	00000000
(1800)	000 0000	00000000	00000000	00000000	00000000	00000000	00000000	00000000	00000000	00000000
(1840)	0 0 0000	00000000	00000000	00000008	00000000	00000000	00000000	00000000	00000000	00000000
(1880)	000 0000	10000000	00000000	00000000	00000000	00000000	00000000	00000000	00000000	00000000
(1920)	000 0000	00000000	00000000	00000000	00000000	00000000	00000000	00000000	00000000	00000000
(1960)	000 0000	00000000	00000000	00000000	00000000	00000000	00000000	00000000	00000000	00000000
(2000)	000 0000	00000000	00000000	00000000	00000000	00000000	00000000	00000000	00000000	00000000
(2040)	000 0000	00000000	00000000	00000000	00000000	00000000	00000000	00000000	00000000	00000000
(2080)	000 0000	00000000	00000000	00000000	00000000	00000000	00000000	00000000	00000000	00000000

```
(  7080)  115E5E5A  5A555252  52D0D5D5  D7D85555  595D5252  545E5E04  0430025A  5A5B5B07  02000013  13171512
(  7120)  124E0313  4F0F1B19  191E0303  031C0C0C  19063A3A  3A030909  0808C0C0  0A0E0139  393A0038  383835 0F
(  7160)  02020208  08053C0B  0A0A0202  2B2B2323  13393939  39343535  3535090F  0F0F0F34  3A3C3C04  04043F3F
(  7200)  3B3B333E  3E010606  06370E38  38380001  05050535  353F3F3F  3F0C0907  07070606  17171717  39383838
(  7240)  383F3F1B  34343732  32370A1A  030D0D36  01053D3D  3D053C07  07070707  042E2424  2424303C  06060606
(  7280)  1140131 3  13132E2A  28353535  350303 03  1130 0908  0808080 8  3D393535  393E3E33  32323230  3C3C3C01
(  7320)  073C3C3D  3D3D3D0A  2E373737  37373434  3C060606  06063A3A  3A3A0105  0D0D0D0D  0D0F3607  07070707
(  7360)  0302020 2  3C0303 05  3A3A3A3A  3A353833  3B3B3B3B  00003A3A  3A0C0A01  010B0B0B  0B0B0B08  073F3F3F
(  7400)  3F3F3E13  13030313  063B3B3E  3E3E3E3E  3E010303  02080808  080F0E0E  0E0E0E0E  03000202  02020202
(  7440)  0D080801  000F0F0F  0A0A0A0A  1E2C2C2C  2D2E2E2E  31 0D0D0D  0A0A0A13  130B0B07  07010108  17171710
(  7480)  1515151F  031F0000  07071313  12121A1F  1F141402  02020216  1E1E1E1A  1C1C1B1B  1F1F0002  02020018
(  7520)  181F01 15  180C3D3D  3D0C0C0C  0C07 0B0B  0606 0618  1F1F1F0E  0505 0509  09 0F3A  3A3A1414  14140202
(  7560)  073F3F3F  3F393939  0012020 2  3E3E3E05  05333338  3030 3C31  310F010E  0E0E1B14  113E3131  31333832
(  7600)  0C0C0C05  07073333  39363234  343E3E02  0430303A  3A393B07  07000007  13171512  12130303  030F1 B1 B
(  7640)  191E1D03  031C0C0C  0C060C3A  3A033109  093D0C0C  0C0A3939  3939003E  3838350A  0F020208  08080503
(  7680)  1A0A0A12  2B2B2B2B  143E3939  39293435  3535 0909  0F0F0F34  343A3C04  0404443F  3B3B3B3B  3E010606
(  7720)  06060E38  38383801  05 05 05 05  393F3F3F  3F3F0907  07070 7CF  17171717  17383838  38383F0B  34343434
(  7760)  3237 0A0A  3A030D36  01010 13D  3D053333  07070707  04382E24  24242630  06060606  06031313  13131325
(  7800)  28283535  35350303  01 1B 0B 19  08 08 0831  3D3D3939  39393E32  32323232  323C3C01  0707073C  3D3D3D0A
(  7840)  192E3737  37373734  32 6 0 6 6  46 06063A  3A3A0101  0505 0D0D  0D0D3605  07070707  07030302  3C030303
(  7880)  05053A3A  3A3A3A05  3B3B3B3B  3B3B003A  3A0C0A0A  0A010B0B  0B0B0B0B  0B323F3F  3F3F3F3E  3E030303
(  7920)  06000033  3E3E3E3E  3E3E3E01  02080808  08080F0E  0E0E0E0E  0E010202  02020202  E0000000  00000000
(  7960)  00000000  00000000  00000000  00000000  00000000  00000000  00000000  00000000  00000000  00000000
(  8000)  000 0000  00000000  00000000  00000000  00000000  00000000  00000000  00000000  00000000  00000000
(  8040)  000 0000  00000000  00000000  00000000  00000000  00000000  00000000  00000000  00000000  00000000
(  8080)  000 0000  00000000  00000000  00000000  00000000  00000000  00000000  00000000  00000000  00000000
(  8120)  000 0000  00000000  00000000  00000000  00000000  00000000  00000000  00000000  00000000  00000000
(  8160)  000 0000  00000000  00000000  00000000  00000000  00000000  00000000  00000000
```

FILE	INPUT RECS.	DATA RECORDS INPUT	MAX. SIZE	READ ERROR SUMMARY PERM	ZERO B	SHORT	UNDEF.	INPUT RETRIES #RECS.	TOTAL#
2	1325	1326	8192	0	0	0	0	0	0

EOJ DUMP STOPPED AFTER FILE 2 # OF PERMANENT READ ERRORS 0

START TIME 10/10/90 23:39:24 STOP TIME 10/10/90 23:41:19

$$

2.287544857713125	-8.079526845685834 5E-02	-0.3906923184731982
1.180131131092457E-02	-658497600.0000000	172800.0000000000
95.69160685472930	64.71419485525813	-65.12618143367140
-19.30135588485299	2.808662002089617	3.649021095900105
12.67260086655233	-1.219550762872672	-5.302919008961579
0.2924492696832132	0.9047198518831246	-4.158069099827904E-02
-0.4001576867069351	115.4980100215927	41.15741974239555
-25.70887273500033	-6.856170486793302	-9.517895147002632
1.820993701512961	8.448019524429744	-0.5359907813153735
-2.300345911099478	8.669678209127720 1E-02	0.3341985519882810
1.192754270672543	55.52133410627954	18.71549961419708
-12.46043777278681	-3.282817659674405	-4.485513022786450
1.086788024917159	4.006627861160525	-0.3442881017478818
-1.091493420754578	5.641093455617725 4E-02	0.1585860323435713
-658152000.0000000	172800.0000000000	-46.48782045767155
-129.0101213893644	29.95804153101349	20.40442088727378
5.000661444491369	12.18887042694623	-3.247872052112057
-9.408310867625777		
100		
1.020228128063511	2.527451275438675	-0.1656202864466886
-0.3663590400678010	91.06803102940192	-79.67459113604821
-51.28510723939785	1.094046092458848	-1.466546983607609
4.115661985555479	11.85999020902407	-1.703712356019009
-4.777888548700274	0.4102151946192766	0.8107875621794091
-5.825932775919254 4E-02	42.61287057292288	-39.44610628148157
-23.91161439750138	0.7253419130562245	-0.6627055847808683
2.180135858173187	5.605079677590742	-0.9698739772632716
-2.260558664813278	0.2376701259563589	0.3836750290802610
-3.387187231903992 0E-02	-657806400.0000000	172800.0000000000
-58.79798840638819	28.92872184087381	-31.06056726737039
5.140268167101323	12.26644524506859	-5.466382446799019
-13.73685243248396	2.571544725714605	5.249740268914877
-0.6441560714356578	-0.8849901182244000	9.222147412265729 2E-02
-20.64629159894399	20.64961848178749	3.567267045578398
-12.12235283275 96	5.592162551487636	13.64251141875074
-3.588240795670248	-8.562118307254056	1.207482860408050
2.259686991897946	-0.1990427923275549	-0.3266349630807405
-10.67826005689948	10.12841766563826	1.362046904869513
-5.752124298687349	2.841201128132630	6.432899046837286
-1.936663411492566	-4.039878276798557	0.6628217388674608
1.066325429182266	-0.1096039541059264	-0.1541396154205384
-657460800.0000000	172800.0000000000	-24.20753710373343
82.02756269987573	47.28743689157824	2.057143994028133
-6.472399911633614	-15.30427058004613	4.511976659987923
9.368569307806646	-1.697635752206589	-2.453280856128821
0.2859638697291837	0.3540751090919003	-87.58213246337426
-83.95761545111846	14.80000928281953	13.94550062502321
10.16682428253574	-4.727184407377277	-12.43976188233074
2.710947882254331	4.676380938444422	-0.7131011359871713
-0.7856695357084821	0.1030550502338635	-41.86721475286764
-38.60864943469301	7.510953752882400	6.554136409477338
4.787309404682066	-2.485248645543408	-5.858186543026145
1.446254295543319		
100		
2.200728271178412	-0.3806498123736706	-0.3696924685202433
5.501255179527447 3E-02	-657115200.0000000	172800.0000000000
119.5271002179726	-47.97010628833575	-55.31141641705711
17.54768516719999	-7.436339173321444	3.149439383002176
13.22107119087019	-3.492689637529669	-5.029965275487099
0.9651906332860420	0.8461216038519151	-0.1405514391428859

B14

D-79980

D-79980 VG2_J_PDS_4_48_USEC.DAT

425952000.000	106.496	6.367	228.611
425952048.000	106.489	6.367	229.094
425952096.000	106.483	6.367	229.577
425952144.000	106.477	6.367	230.060
425952192.000	106.470	6.367	230.543
425952240.000	106.464	6.367	231.026
425952288.000	106.458	6.367	231.509
425952336.000	106.452	6.367	231.992
425952384.000	106.445	6.367	232.474
426802672.000	286.047	5.292	252.096
426802720.000	286.053	5.292	252.579
426802768.000	286.059	5.292	253.063
426802816.000	286.064	5.292	253.547
426802864.000	286.070	5.292	254.030
426802912.000	286.076	5.292	254.514
426802960.000	286.081	5.292	254.997
426803008.000	286.087	5.292	255.481
426803056.000	286.092	5.292	255.964